

Generation of bright laser-like coherent emissions from nitrogen molecular ions in intense infrared laser fields: A unique quantum system for extreme nonlinear optics

Jinping Yao¹, Wei Chu¹, Zhaoxiang Liu^{1,2}, Bo Xu^{1,2}, Jinming Chen^{1,2,3}, and Ya Cheng^{1,4,5,*}

¹*State Key Laboratory of High Field Laser Physics, Shanghai Institute of Optics and Fine Mechanics, Chinese Academy of Sciences, Shanghai 201800, China*

²*University of Chinese Academy of Sciences, Beijing 100049, China*

³*School of Physical Science and Technology, ShanghaiTech University, Shanghai 200031, China*

⁴*State Key Laboratory of Precision Spectroscopy, East China Normal University, Shanghai 200062, China*

⁵*Collaborative Innovation Center of Extreme Optics, Shanxi University, Taiyuan, Shanxi 030006, China*

*ya.cheng@siom.ac.cn

Abstract

We report on an investigation of simultaneous generation of several narrow-bandwidth laser-like coherent emissions from nitrogen molecular ions (N_2^+) produced in intense mid-infrared laser fields. With systematic examinations on the dependences of N_2^+ coherent emissions on gas pressure as well as several laser parameters including laser intensity, polarization and wavelength of the pump laser pulses, we reveal that the multiple coherent emission lines generated in N_2^+ originate from a series of nonlinear processes beginning with four-wave mixing, followed with stimulated Raman scattering. Our analyses further show that the observed nonlinear processes are greatly enhanced at the resonant wavelengths, giving rise to high conversion efficiencies from the infrared pump laser pulses to the coherent emission lines near the transition wavelengths between the different vibrational energy levels of ground $N_2^+(X^2\Sigma_g^+)$ and that of the excited $N_2^+(B^2\Sigma_u^+)$ states.

PACS numbers: 42.65.Re, 42.65.Ky

The advent of ultrashort and ultraintense laser pulses has revolutionized the interaction of light with matter. Owing to the ultrashort pulse durations and ultrahigh peak intensities, photoionization of atoms and small molecules, which are the building blocks of most matter, in intense ultrashort laser fields is strongly suppressed in the rising edge before the approach of the crest of the pulses. This characteristic creates a unique condition of extreme nonlinear photoionization for which the perturbative nonlinear theory fails due to the comparable strengths of light field and Coulomb field. The non-perturbative photoionization process can be nicely described by a tunnel ionization picture which is the pillar stone of strong field laser physics [1]. With the tunnel ionization as the initiative process, highly nonlinear processes such as high-order harmonic generation [2], above threshold ionization [3], and non-sequential double-ionization [4] have been observed, which further provide the means to access the dynamics in atomic and molecular systems on attosecond time scale. Nowadays, attosecond physics has become one of the most active areas of modern physics.

Recently, lasing actions induced by tunnel ionization of nitrogen molecules have been observed which come as a major surprise to those who have been investigating strong field physics over the past three decades [5-21]. These observations were made with either a pump laser at 800 nm wavelength [6,8-20] or that at longer wavelengths in the range from 1 μm to 4 μm [5,7,21]. A common characteristic in these experiments reported so far is that to initiate the lasing actions, either external or self-generated seed pulses must be involved to trigger the stimulated emissions observed exclusively in the forward direction. Therefore, it would be logical to expect that generation of the lasers from the nitrogen molecular ions (N_2^+) produced in strong laser fields should share a same mechanism regardless of the wavelengths of the pump lasers.

However, further pump-probe investigations on the generation of N_2^+ lasers at 391.4 nm, which corresponds to the transition between $\text{N}_2^+(\text{B}^2\Sigma_u^+, v'=0)$ and $\text{N}_2^+(\text{X}^2\Sigma_g^+, v=0)$ states, at different pump wavelengths clearly show that the gain of the external seed pulses whose

spectra overlap the 391.4 nm transition line can only be observed for the pump laser at 800 nm wavelength but not the other wavelengths in the infrared range [18]. The experimental results lead to two consequences as follows. First, the nitrogen molecular ions produced in the 800 nm fields are preferentially populated on the excited $N_2^+(B^2\Sigma_u^+, v'=0)$ state but not the ground $N_2^+(X^2\Sigma_g^+, v=0)$ state, resulting in a population inversion which is difficult to understand in the framework of tunnel ionization [1,18]. Second, there should be no population inversion in nitrogen molecular ions produced in laser fields at infrared wavelengths ranging from 1 μm to 4 μm as evidenced by the failure of observing any gain in the external seed pulses injected immediately after the pump pulses to avoid temporal overlap between the two [18]. The origin of the laser-like emissions observed only with the self-generated seed pulses (i.e., the harmonics of the pump laser) at pump wavelengths longer than 1 μm is another puzzle yet to be unlocked.

Although the first question, which relates to generation of the N_2^+ lasers with the 800 nm pump pulses, has been intensively investigated in the past a few years [6,8-20], the second question above has not yet aroused sufficient attention [5,7,21], most likely due to the short history of this new branch of research. In fact, understanding how the N_2^+ lasers are generated with the pump pulses of longer wavelengths is critical for providing the complete physical picture behind this intriguing phenomenon. This motivates us to perform a systematic investigation on the generation of N_2^+ lasers at various pump wavelengths in the range of 1.2 μm and 2 μm , which is the wavelength range of our OPA source. Surprisingly, our observations indicate that some conclusions drawn from the previous experiments are not always true. Among the deviations, the most significant two features reported here are (1) generation of the N_2^+ lasers can be achieved even when the spectra of seed pulses do not overlap the observed N_2^+ laser wavelengths, and (2) the laser lines can be significantly broadened to form a supercontinuum-like spectrum with a bandwidth of ~ 80 nm at low gas pressures. These findings provide vital clues for understanding the extreme nonlinear interactions between the strong laser fields and nitrogen molecular ions.

The experiments were carried out using an optical parametric amplifier (OPA, HE-TOPAS, Light Conversion Ltd.), which was pumped by a commercial Ti:sapphire laser system (Legend Elite-Duo, Coherent, Inc.). The OPA enables to generate wavelength-tunable femtosecond laser pulses in the range from 1.2 μm to 2.4 μm at a repetition rate of 1 kHz. Two pairs of 0.5 mm-thickness glass plates were inserted in the path of pump beam to control the pulse energy of the pump laser by changing the incident angles. The pump laser pulses were then focused into the gas chamber filled with nitrogen gas using an $f=10$ cm lens, and were further collimated using another lens with the same focal length. The signal beam exiting from the gas chamber together with the pump laser were attenuated by Fresnel reflection with a piece of uncoated glass plate. Afterwards, the residual pump laser was eliminated with a piece of blue glass. At last, the generated third and fifth-order harmonic beams were focused into a grating spectrometer (Shamrock 303i, Andor) by a lens with a focal length of 15 cm. The intensity of the signal beam was adjusted by several variable attenuation filters placed in series before the spectrometer. The spectra of the fundamental waves before and after passing through the gas chamber were measured by a fiber spectrometer (NIRQuest512, Ocean Optics, Inc.) with an integration sphere.

Figure 1(a) shows the dependence of the spectra of several N_2^+ emission lines on the gas pressure of nitrogen molecules obtained with pump pulses at a wavelength of 1580 nm. The pump power and the beam diameter ($1/e^2$ width) are approximately 1.0 W and 7.6 mm, respectively. It is noteworthy that in such a case, neither the third nor the fifth harmonic of the pump laser could cover the transition lines at either 358.2 nm or 391.4 nm wavelengths. Surprisingly, two strong coherent emissions appear near the two transition lines at 358.2 nm and 391.4 nm wavelengths, which correspond to $\text{N}_2^+(\text{B}^2\Sigma_u^+, v'=1) \rightarrow \text{N}_2^+(\text{X}^2\Sigma_g^+, v=0)$ and $\text{N}_2^+(\text{B}^2\Sigma_u^+, v'=0) \rightarrow \text{N}_2^+(\text{X}^2\Sigma_g^+, v=0)$, respectively. Meanwhile, a weak emission at ~ 331 nm also appears on the fifth harmonic spectrum, which corresponds to the transition $\text{N}_2^+(\text{B}^2\Sigma_u^+, v'=2) \rightarrow \text{N}_2^+(\text{X}^2\Sigma_g^+, v=0)$. At high gas pressures above 40 mbar, the coherent emissions are mostly of narrow-bandwidths which is the typical feature in fifth harmonic generation in many gaseous media under our laser condition. The relatively high gas

pressure will prevent the buildup of high peak intensity due to the plasma defocusing. However, at lower gas pressures in the range from 10 mbar to 30 mbar, pronounced supercontinuum spectra have been observed which fill up the gap between ~ 331 nm and ~ 358 nm as well as that between ~ 358 nm and ~ 391 nm. Naturally, one would expect that the supercontinuum generated near the transition lines of N_2^+ is a characteristic related to the energy level structure of molecular ions. We have confirmed this by carrying out a comparative experiment in argon, as argon has an ionization potential and a nonlinear coefficient similar to that of the nitrogen molecules [22]. In this case, all of the experimental conditions remained the same except that the gas in the chamber was changed from nitrogen molecules to argon atoms. The fifth harmonic spectrum generated in argon as a function of the gas pressure is shown in Fig. 1(b), which shows a smooth spectrum with a reasonable bandwidth of 9~10 nm (FWHM) and centered at the wavelength of ~ 319 nm (i.e., close to one fifth of the pump wavelength). The bright narrow-bandwidth emissions as well as the supercontinua both disappear in the spectrum in Fig. 1(b).

An immediate thought after seeing the spectrum in Fig. 1(a) would be that such unusual fifth harmonic spectra should be a result of the strong distortion in the spectra of pump pulses and/or the third harmonic wave caused by nonlinear spectral broadening. Therefore, we measured the spectra of the pump pulses and the third harmonic in both nitrogen and argon gases at different gas pressures. As shown in Fig. 2(a-d), both the spectra in nitrogen and argon are very similar without any noticeable differences. From Fig. 2(a) and (c), one can see that below 30 mbar, the spectra of the pump pulses are undergoing a continuous blue shifting as well as a spectral broadening with the increase of the gas pressure. The blue shift can be attributed to the plasma generation as have been intensively discussed in previous investigations [23]. Above 30 mbar, the spectral broadening becomes more pronounced than the blue shift. For the third harmonic signals, the intensities increase with the increasing gas pressure, and the spectra broaden as well, as shown in Fig. 2(b) and (d). Nevertheless, both the pump laser at the fundamental wavelength and the generated third harmonic signal show limited increases in the spectral bandwidths which are much less pronounced than that of the fifth harmonic in Fig. 1(a). Thus, we exclude the possibilities

of directly generating the supercontinuum via the fifth harmonic generation in the pump laser field.

To gain insight into the physical mechanism behind the result in Fig. 1(a), we further investigate the dependences of the fifth harmonic signals generated in nitrogen molecules on the intensity, polarization and wavelength of the pump laser. Figure 3(a) shows the supercontinuum spectra measured at different pump laser intensities for a fixed gas pressure of 16 mbar. Here, to tune the laser intensity in the gas, we varied the power of the pump laser by changing the incident angle of the pump laser beam at two pairs of thin glass plates. The supercontinuum already began to appear at a relatively low pump power of 200 mW, corresponding to a peak intensity of $\sim 3 \times 10^{14}$ W/cm² as evaluated by assuming linear propagation of the pump laser in the gas chamber. When the pump laser intensity increased, the supercontinuum became stronger and its spectrum became broader. Then, we changed polarization of the pump laser at an average power of ~ 1 W from linear to circular using an achromatic quarter-wave plate (QWP) at the optimized gas pressure of 16 mbar. Here, the angle of 0° corresponds to linear polarization, and the angles of $\pm 45^\circ$ correspond to circular polarization. Since the Fresnel reflection from the uncoated glass plate is sensitive to the polarization of the incident light, we replaced the uncoated glass plate placed after the gas chamber with a broad-band reflective mirror which is insensitive to the laser polarization. As shown by Fig. 3(b), the supercontinua generated with the linearly polarized pump lasers are the strongest in its intensity and the broadest in its spectrum. In contrast, changing the polarization of pump pulses from linear to circular polarization leads to a significant drop of the signal intensities by 3~4 orders of magnitude.

Another important feature of the supercontinuum generation is its dependence on the pump wavelength. To clarify this, we examined the supercontinuum generation at two additional pump wavelengths of 1780 nm and 1400 nm, which are presented in Fig. 3(c) and (d), respectively. The pump powers at 1780 nm and 1400 nm were approximately 0.83 W and 1.0 W, respectively, which are the maximum output powers of our OPA system at the two wavelengths. The beam diameters ($1/e^2$ width) were measured to be 9.3 mm and 6.2 mm for the 1780 nm and 1400 nm pump laser, respectively. It is noteworthy that a series of

attenuation filters were adjusted to obtain high signal-to-noise ratios at all the pump wavelengths. For this reason, the intensities of the N_2^+ lasers measured at different pump wavelengths are not calibrated. It was observed that at the pump wavelength of 1780 nm, the coherent emissions at ~ 391 nm and ~ 358 nm can be both efficiently generated as evidenced by Fig. 3(c), with a supercontinuum filling up the gap between the two emission lines. Although strong coherent emission at ~ 428 nm corresponding to the transition $N_2^+(B^2\Sigma_u^+, v'=0) \rightarrow N_2^+(X^2\Sigma_g^+, v=1)$ is also observed, no supercontinuum is observed between the laser lines at ~ 391 nm and ~ 428 nm. Meanwhile, some weak emissions from the transitions between the high vibrational energy levels of $N_2^+(B^2\Sigma_u^+)$ and that of $N_2^+(X^2\Sigma_g^+)$ states appears in the spectral range of 410~420 nm. In contrast, switching the pump wavelength from 1780 nm to 1400 nm leads to an almost complete elimination of the coherent emissions at ~ 391 nm and ~ 358 nm as well as the supercontinuum in between, as shown in Fig. 3(d). In such a case, only a strong emission at ~ 428 nm appears on the third harmonic spectrum. The results in Fig. 1(a), Fig. 3(c) and (d) indicate the important role of the pump wavelength in the generation of the supercontinuum and N_2^+ coherent emissions, which is discussed below to facilitate establishing a physical model towards complete understanding of the observations described above.

The key message from the results in Fig. 1 and Fig. 3 is that the generation of the N_2^+ lasers at ~ 391 nm and ~ 358 nm wavelengths can only be achieved when the spectra of seed pulses overlap one of the transition lines between $N_2^+(B^2\Sigma_u^+)$ and $N_2^+(X^2\Sigma_g^+)$ states. This feature suggests that the fifth harmonic generation, which produces the seed pulses, has been enhanced as a result of some resonant nonlinear processes. Since the fifth-order nonlinear susceptibility ($\chi^{(5)}$) is usually much smaller than the three-order susceptibility ($\chi^{(3)}$), the fifth harmonic can be near resonantly generated through a cascaded third-order nonlinear process of $5\omega=3\omega+\omega+\omega$, giving rise to photons at ~ 331 nm whose spectrum is shown in Fig. 1(a). The process is schematically depicted in Fig. 4(a). We would like to stress that

due to the high peak intensity of pump pulses, the near-resonant process in Fig. 4(a) can be very efficient thanks to its highly nonlinear dependence on the pump laser intensity.

Subsequently, the generated 5ω photons at ~ 331 nm can initiate a Raman process in the excited nitrogen molecular ions, as illustrated by a pair of the arrow-headed solid lines in purple and green colors as depicted in Fig. 4(b), which leads to the generation of photons at ~ 358 nm wavelength. The vibrational Raman process can be initiated within the duration of pump laser because the vibrational period of $N_2^+(B^2\Sigma_u^+)$ state (i.e., ~ 14 fs) is shorter than the pulse duration of the pump laser (i.e., ~ 60 fs). Once the coherent emission at ~ 358 nm wavelength is generated, it triggers further Raman process to produce the photons at ~ 391 nm wavelength, as depicted in Fig. 4(b) with a pair of arrow-headed dashed lines in green and fuchsia colors.

One may argue that the efficiency of spontaneous Raman scattering, generally speaking, is low. On the other hand, both the emission lines at ~ 358 nm and ~ 391 nm observed in our experiment appears strong with their intensities comparable to that of the fifth harmonic signal. To understand the point, we must realize that the nitrogen molecular ions under the investigation are a unique system which allows the resonant transitions as depicted in Fig. 4(c) to occur, mediated by the Raman photons generated in Fig. 4(b). We provide an understanding of the circumstance from the classical picture of Raman process as follow. After the generation of a coherent emission at ~ 331 nm wavelength with the resonant three-photon process, the processes in Fig. 4(b) will further produce the Stokes photons at ~ 358 nm and ~ 391 nm wavelengths by Raman scattering. The initial Raman scattering processes can be enhanced to have decent conversion efficiencies due to the fact that the molecular ions prepared on the excited states should have higher nonlinear coefficients than that of molecular ions on the ground state [24,25]. Subsequently, the initially generated Stokes photons at ~ 358 nm and ~ 391 nm wavelengths will be absorbed by the nitrogen molecular ions which are mostly populated on the ground state (i.e., there is no population inversion) as a result of the resonant transitions, as illustrated in Fig. 4(c). The processes in Fig. 4(c) in turn give rise to higher populations in the vibrational states $v'=0$ and $v'=1$ of the excited

$N_2^+(B^2\Sigma_u^+)$ state. Essentially, it is the beating between these two coherent vibrational wavepackets which leads to an oscillating optical polarizability of the molecular nitrogen ions at the vibrational frequency of $\Delta v'=1$. The processes in Fig. 4(b) and Fig. 4(c) can therefore reinforce each other in the sense that the enhanced oscillation in the optical polarizability induced by the processes in Fig. 4(c) will in turn promote the efficiencies of both Raman processes in Fig. 4(b). This mechanism is similar to that behind the stimulated Raman scattering. The difference is that the traditional stimulated Raman scattering does not involve any resonant electronic states. From this point of view, the strong emission lines at ~ 358 nm and ~ 391 nm are a result of stimulated Raman scattering from the excited molecular ions mediated by the resonant transitions between the ground $N_2^+(X^2\Sigma_g^+)$ and excited $N_2^+(B^2\Sigma_u^+)$ states.

The last question is how the supercontinua between the stimulated Raman lasing lines are generated although the supercontinua are not resonant with any transitions between the ground $N_2^+(X^2\Sigma_g^+)$ and excited $N_2^+(B^2\Sigma_u^+)$ states. We notice that our experiments are carried out using tight focusing. Together with the high pulse energies and low gas pressures, high peak intensities can be reached in the low-density nitrogen molecular ions, as the plasma defocusing is insignificant under the low gas pressure. Therefore, cross phase modulation can occur immediately after the generation of the stimulated Raman lasers in the intense pump laser fields. In particular, the narrow-bandwidth Raman lines near 358 nm and 391 nm wavelengths are in resonances with the transitions between the ground $N_2^+(X^2\Sigma_g^+)$ and excited $N_2^+(B^2\Sigma_u^+)$ states. In such case, the efficiency of cross phase modulation will be greatly enhanced, leading to the extraordinary supercontinuum generation which is rarely observed with atomic or neutral molecular gases under the similar experiment conditions. Because the cross phase modulation in N_2^+ mainly occurs in the falling edge of the pump pulse (i.e., most ions are produced after the crest of the pump pulses), the spectral blue shift is more pronounced than red shift. The process is schematically depicted in Fig. 4(d). It is noteworthy that when the pump wavelength is switched from 1580 nm to 1780 nm, a nonlinear process similar to that in Fig. 4(a-d) would

dominate the generation for both the lines at ~ 358 nm and ~ 391 nm wavelengths as well as the supercontinuum in between. That is to say, the coherent emission near 358 nm wavelength is generated through the process of $5\omega=3\omega+\omega+\omega$, whilst the coherent emission near 391 nm wavelength is the Stokes photons produced by the stimulated Raman scattering. For the pump laser at 1400 nm, although its third harmonic spectrum can cover the transition line at ~ 428 nm, the above mechanism illustrated in Fig. 4(a-c) will not apply due to the photon energy mismatch between the stimulated Raman process in the excited N_2^+ ions and the resonant single-photon absorption between the ground $N_2^+(X^2\Sigma_g^+)$ and excited $N_2^+(B^2\Sigma_u^+)$ states, which is in good agreement with our observation in Fig. 3(d).

To conclude, we have investigated near-resonant extreme nonlinear optics in nitrogen molecular ions produced in strong laser fields at several wavelengths between 1.2 μm and 2 μm . Due to the existence of abundant vibrational energy levels, a series of third-order nonlinear optical processes including three photon excitation, stimulated Raman scattering, and cross phase modulation can occur almost simultaneously at multiple resonant wavelengths. We notice that nitrogen molecular ions are a unique quantum system for demonstrating such extreme nonlinear effects. Since these molecular ions have a large ionization potential as high as ~ 28 eV, they can survive against photoionization at visible and infrared (IR) wavelengths even when the pump laser intensity reaches 8.5×10^{14} W/cm² (assuming an ionization probability of $\sim 1\%$). In the meantime, the nitrogen molecular ions can also allow the resonant transitions between various vibrational levels of the ground $N_2^+(X^2\Sigma_g^+)$ and excited $N_2^+(B^2\Sigma_u^+)$ states to occur at near ultraviolet (UV) wavelengths, which can be resonant with the third or fifth harmonics of the IR pump laser. The rich phenomena observed in the unique quantum system suggest that the extreme nonlinear optics in molecular ions will not only become an intriguing topic of research for further exploration but also hold great promise for air-laser-based remote sensing applications.

This work is supported by the National Basic Research Program of China (Grant No. 2014CB921303), National Natural Science Foundation of China (Grant Nos. 61575211,

11674340, 61405220 and 11404357), Research Programs of the Chinese Academy of Sciences (Grant Nos. XDB16000000, QYZDJ-SSW-SLH010), and Shanghai Rising-Star Program (Grant No. 17QA1404600).

References:

- [1] L.V. Keldysh, Zh. Eksp. Teor. Fiz. **47**, 1945 (1964) [Sov. Phys. JETP **20**, 1307 (1965)].
- [2] A. L’Huillier and Ph. Balcou, Phys. Rev. Lett. **70**, 774–777 (1993).
- [3] K. J. Schafer, Baorui Yang, L. F. DiMauro, and K. C. Kulander, Phys. Rev. Lett. **70**, 1599–1602 (1993).
- [4] A. l’Huillier, L. A. Lompre, G. Mainfray, and C. Manus, Phys. Rev. A **27**, 2503–2512 (1983).
- [5] J. Yao, B. Zeng, H. Xu, G. Li, W. Chu, J. Ni, H. Zhang, S. L. Chin, Y. Cheng, and Z. Xu, Phys. Rev. A **84**, 051802(R) (2011).
- [6] Q. Luo, W. Liu, and S. L. Chin, Appl. Phys. B **76**, 337–340 (2003).
- [7] D. Kartashov, J. Möhring, G. Andriukaitis, A. Pugžlys, A. Zheltikov, M. Motzkus, and A. Baltuška, CLEO:QELS-Fundamental Science, OSA Technical Digest QTh4E.6 (2012).
- [8] J. Yao, G. Li, C. Jing, B. Zeng, W. Chu, J. Ni, H. Zhang, H. Xie, C. Zhang, H. Li, H. Xu, S. L. Chin, Y. Cheng, and Z. Xu, New J. Phys. **15**, 023046 (2013).
- [9] H. Zhang, C. Jing, J. Yao, G. Li, B. Zeng, W. Chu, J. Ni, H. Xie, H. Xu, S. L. Chin, K. Yamanouchi, Y. Cheng, and Z. Xu, Phys. Rev. X **3**, 041009 (2013).
- [10] Y. Liu, Y. Brelet, G. Point, A. Houard, and A. Mysyrowicz, Opt. Express **21**, 22791–22798 (2013).
- [11] T. Wang, J. F. Daigle, J. Ju, S. Yuan, R. Li, and S. L. Chin, Phys. Rev. A **88**, 053429 (2013).
- [12] J. Ni, W. Chu, C. Jing, H. Zhang, B. Zeng, J. Yao, G. Li, H. Xie, C. Zhang, H. Xu, S. L. Chin, Y. Cheng, and Z. Xu, Opt. Express **21**, 8746–8752 (2013).
- [13] G. Point, Y. Liu, Y. Brelet, S. Mitryukovskiy, P. Ding, A. Houard, and A. Mysyrowicz, Opt. Lett. **39**, 1725–1728 (2014).
- [14] B. Zeng, W. Chu, G. Li, J. Yao, H. Zhang, J. Ni, C. Jing, H. Xie, and Y. Cheng,

- Phys. Rev. A **89**, 042508 (2014).
- [15] Y. Liu, P. Ding, G. Lambert, A. Houard, V. Tikhonchuk, and A. Mysyrowicz, Phys. Rev. Lett. **115**, 133203 (2015).
- [16] P. Wang, C. Wu, M. Lei, B. Dai, H. Yang, H. Jiang, and Q. Gong, Phys. Rev. A **92**, 063412 (2015).
- [17] H. Xu, E. Lötstedt, A. Iwasaki, and K. Yamanouchi, Nature Commun. **6**, 8347 (2015).
- [18] J. Yao, S. Jiang, W. Chu, B. Zeng, C. Wu, R. Lu, Z. Li, H. Xie, G. Li, C. Yu, Z. Wang, H. Jiang, Q. Gong, and Y. Cheng, Phys. Rev. Lett. **116**, 143007 (2016).
- [19] L. Arissian, B. Kamer, and A. Rasoulof, Opt. Commun. **369**, 215–219 (2016).
- [20] M. Lei, C. Wu, A. Zhang, Q. Gong, and H. Jiang, Opt. Express **25**, 4535–4541 (2017).
- [21] A. Azarm, P. B. Corkum, and P. G. Polynkin, in Conference on Lasers and Electro-Optics, OSA Technical Digest (online) (Optical Society of America, 2016), paper JTh4B.9.
- [22] V. Loriot, E. Hertz, O. Faucher, and B. Lavorel, Opt. Express **18**, 3011–3012 (2010).
- [23] S. C. Rae and K. Burnett, Phys. Rev. A **46**, 1084–1090 (1992).
- [24] D. C. Rodenberger, J. R. Heflin, and A. F. Garito, Nature **359**, 309–311 (1992).
- [25] H. Xie, G. Li, J. Yao, W. Chu, Z. Li, B. Zeng, Z. Wang, and Y. Cheng, Sci. Rep. **5**, 16006 (2015).

Captions of figures:

Fig. 1 (Color online) Dependences of the fifth harmonic spectra generated in (a) nitrogen and (b) argon gases with the 1580 nm pump laser on gas pressure. Note that the color bars are in log scale.

Fig. 2 (Color online) Dependences of the spectra of (a) the pump pulses at 1580 nm wavelength after passing through nitrogen gas as well as (b) the generated third harmonic on the gas pressure. For comparison, the corresponding results obtained from argon gas with the same laser conditions are present in (c) and (d), respectively. The color bars are in log scale.

Fig. 3 (Color online) Dependence of the fifth harmonic spectra generated in nitrogen gas at a fixed gas pressure of 16 mbar on (a) intensity and (b) polarization of the 1580 nm pump laser, and the pressure-dependent spectra of the fifth harmonic generated at different wavelengths of (c) 1780 nm and (d) 1400 nm of the pump laser. The color bars are in log scale.

Fig. 4 (Color online) Schematic diagram of the physical mechanism underlying the generation of N_2^+ coherent emissions in the intense IR laser fields. (a) The signal around 331 nm is generated with a near-resonant nonlinear process of $5\omega=3\omega+\omega+\omega$. (b) The signals near 358 nm and 391 nm are generated through stimulated Raman scattering. (c) The one-photon resonant absorptions from $N_2^+(X^2\Sigma_g^+, v=0)$ to $N_2^+(B^2\Sigma_u^+, v'=0,1)$ promotes the populations of nitrogen molecular ions at the ground and first excited vibrational states in the excited electronic state, which in turn enhances the efficiency of stimulated Raman scattering in (b). (d) The emission lines at ~ 358 nm and ~ 391 nm are spectrally broadened by a cross phase modulation assisted by the intense pump laser to produce the supercontinuum. Note that the cross phase modulation occurs in a near-resonant condition which promotes the spectral broadening.

Fig. 1

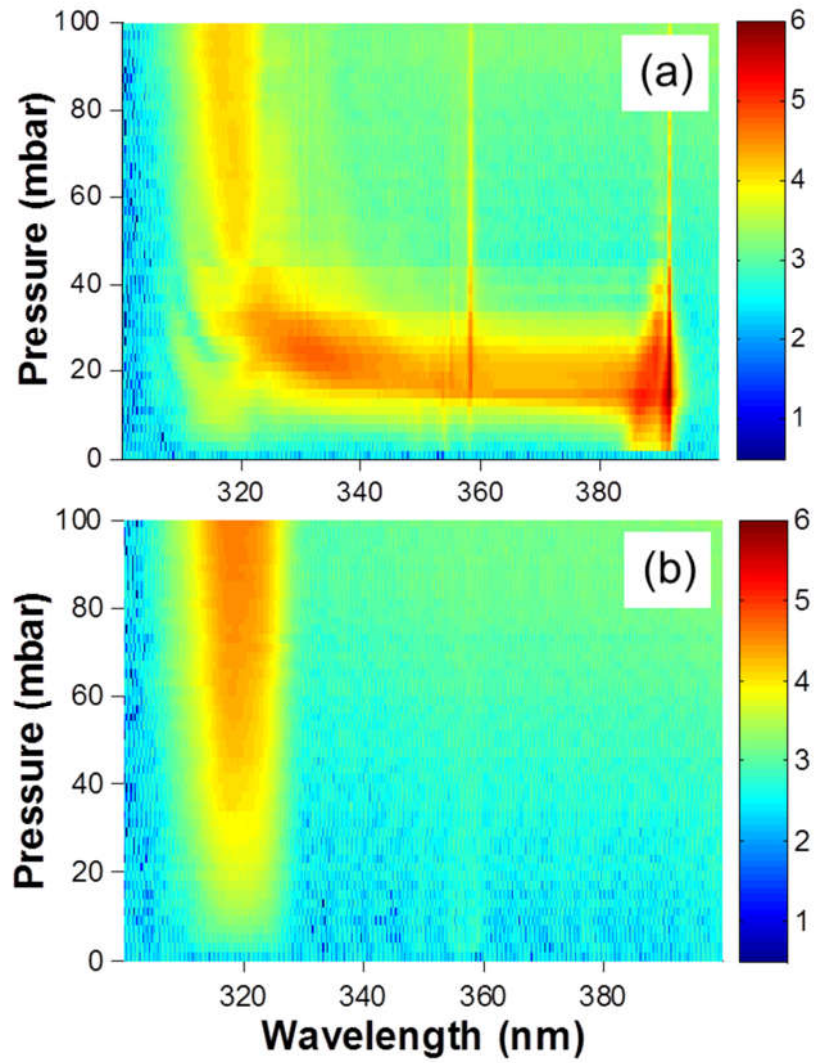


Fig. 2

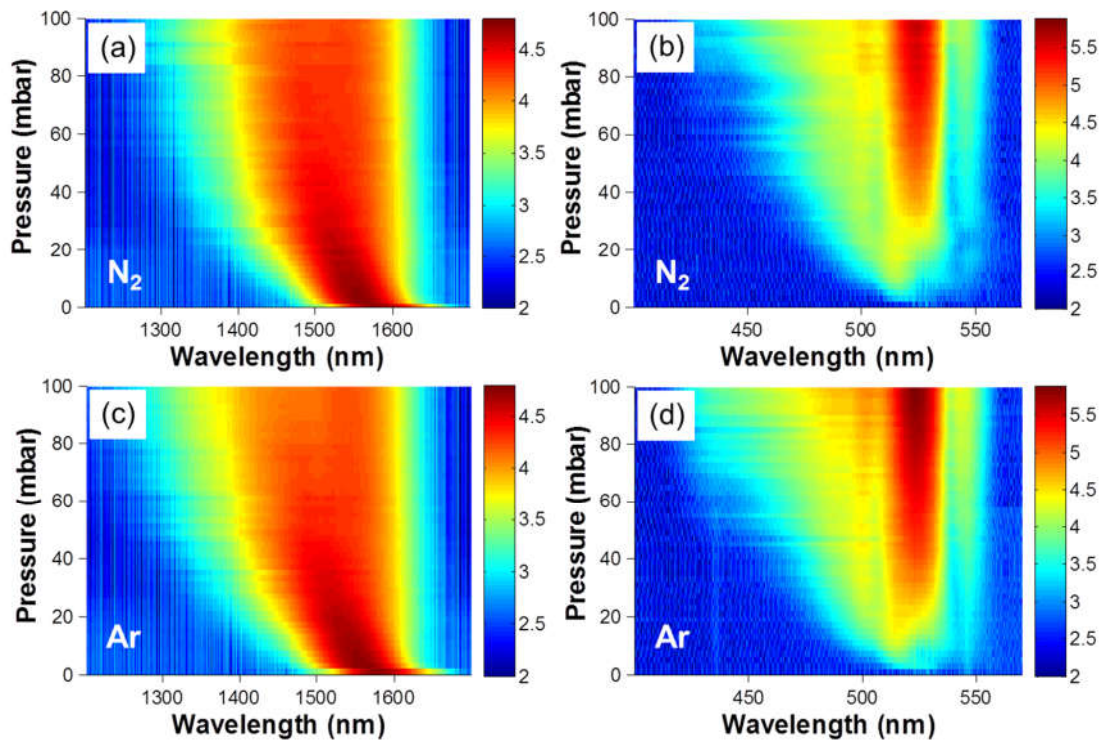


Fig. 3

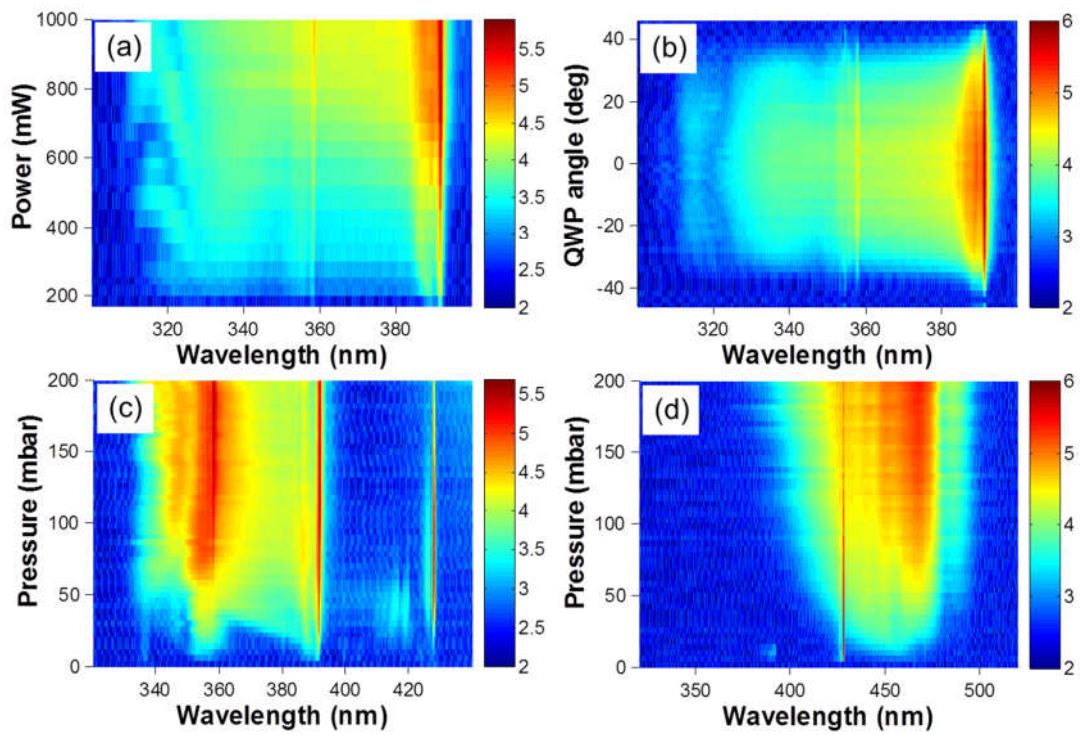


Fig. 4

